УДК 551.324.54

Geodetic observation and interpretation of ice flow velocities in the southern part of subglacial Lake Vostok

© 2012 г. A. Richter[1], D.V. Fedorov[2], S.V. Popov[3], M. Fritsche[1], V.Ya. Lipenkov[4], A.A. Ekaykin[4], V.V. Lukin[4], A.Yu. Matveev[2], R. Dietrich[1]

[1]Technische Universität Dresden, Institut für Planetare Geodäsie, Dresden, Germany;
[2]OAO «Aerogeodeziya», St. Petersburg; [3]Polar Marine Geosurvey Expedition, St. Petersburg;
[4]Arctic and Antarctic Research Institute St. Petersburg
andreas.richter@tu-dresden.de

Статья принята к печати 3 сентября 2012 г.

Accumulation, Antarctica, flow velocity, flux gate, GPS, mass balance.
Аккумуляция, Антарктида, баланс массы, скорость течения, створ ледяного потока, GPS.

Results of geodetic in-situ observations of ice-flow velocities in the southern part of subglacial Lake Vostok are combined with data sets of the ice surface topography, ice thickness, surface accumulation, basal accretion and firn/ice density for interpretations regarding the glaciological setting of the Lake Vostok system. Based on the ice-flow velocities and the ice thickness, mean surface accumulation rates are derived applying the flux gate method. These are representative for surface segments extending from the southern part of Lake Vostok to the Ridge B ice divide. They are consistent with the present-day accumulation rate at Vostok station and its variation upstream and thus suggest that the area has been close to steady state. In addition, ice-flow dynamics are investigated along a flow line segment extending from 26 km upstream to 12 km downstream from Vostok station. The analysis suggests deficiencies in current modelling approaches within the transition zone from floating to grounded ice.

Introduction

The results derived from the deep drilling at Vostok station, and the recent penetration to subglacial Lake Vostok, have impressively demonstrated the wealth and diversity of scientific questions for the answer of which glaciology can play a central role. In this context, geodetic observations and glaciological interpretation are closely linked in the particular setting of the Lake Vostok system. In 2001, an intensive cooperation between the geodesists of Technische Universität Dresden (Germany) and Aerogeodeziya (St. Petersburg), along with the glaciologists from the Arctic and Antarctic Research Institute (St. Petersburg) and the geophysicists of the Polar Marine Geosurvey Expedition (St. Petersburg) and with logistic support of the Russian Antarctic Expedition (RAE, St. Petersburg) was begun with the aim to contribute geodetic results to the exploration of Lake Vostok and its glaciological setting. This cooperation has been and will be continued, including joint field work in the Lake Vostok region, also in the upcoming years.

A brief overview of the results achieved so far by the joint efforts is given in the following section. Section 3 describes the observational data available to date for investigations in the southern part of Lake Vostok. Section 4 comprises two examples for the application of these data with regard to questions of glaciological relevance: First, mean accumulation rates are inferred from flux gates across the ice-flow direction which is representative for surface segments extending from the southern part of Lake Vostok to the Ridge B ice divide. Second, the flow dynamics in the transition zone from floating to grounded ice is investigated along a flow line segment extending from 26 km upstream to 12 km downstream from Vostok station.

Previous works – a review

Ice surface geometry. One geodetic contribution to the investigation of subglacial Lake Vostok consists in the precise determination of the geometry of the ice surface in the region. A refined analysis of satellite radar altimetry data of the ERS-1 mission [9] yielded a high-resolution digital elevation model (DEM) of the ice surface in the Lake Vostok area [23]. More recently, a regional crossover analysis was performed on the satellite laser altimetry data of the ICESat mission [25] resulting in a new regional DEM of the ice surface [13]. Compared to the radar altimetry data, the ICESat data set is characterized by:

a higher accuracy of the altimeter measurements;
a smaller footprint diameter (60–70 m vs. > 2.5 km);
laser altimeter measurements free of the systematic effect of signal penetration (volume backscatter);
high along-track resolution (172 m vs. 350 m);
a wider across-track spacing (up to 20 km vs. 2 km).

The last fact implies an additional increase in the uncertainty of the DEM within the meshes between the satellite tracks, where the elevation values are obtained by interpolation.

Both models were combined to a hybrid DEM [13]. At each ICESat measurement point, the height difference of the interpolated elevation from the radar-derived DEM minus the laser altimeter measurement was determined. Over the lake

area, this difference is very homogeneous (standard deviation 40 cm). The radar-derived elevations are, on average, 1.19 m lower than the laser altimetry data, which is interpreted as the effect of signal penetration of the radar altimeter measurements. The difference (radar minus laser) was interpolated between the ICESat tracks and applied as a correction to the elevations of the radar-derived DEM. In this way, the hybrid DEM was obtained which combines the high spatial resolution of the radar altimetry data with the accuracy of the laser measurements.

This DEM reveals interesting details on the surface relief in the area of Lake Vostok. Of particular interest are the striking troughs along the western (upstream), and bumps along the eastern (downstream) shores of the subglacial lake (see also [19]). The DEM, along with an ice-thickness model and a regional geoid model, was furthermore applied for a quantitative evaluation of the hydrostatic equilibrium of the ice sheet above Lake Vostok [13]. This study showed that most of the ice surface above the subglacial lake fulfils the hydrostatic equilibrium within a few meters. A large positive violation (+10 m) of the hydrostatic equilibrium is found within a fringe along the shore line, which would allow to map a generalized lake contour. Further, local violations of the hydrostatic equilibrium correspond to locations where the ice sheet is grounded on small bedrock islands. Finally, the HE examination revealed an area of anomalous, anthropogenic surface snow densification along the convoy track from Vostok station towards Mirny.

The ice surface above Lake Vostok was also used as a calibration area for the determination of ICESat laser operational period biases [13]. The relative systematic biases can now be applied as corrections to the ICESat data from other ice covered regions to separate this systematic effect from real temporal ice-surface elevation changes.

Ice flow velocities. Another geodetic result of high glaciological relevance consists in the accurate determination of ice flow velocities. Based on repeated GNSS (Global Navigation Satellite Systems, comprising to date GPS and GLONASS) observations on surface markers, horizontal velocity components were derived [21]. These velocity components are given relative to bedrock as the local velocity contribution of the rotation of the Antarctic tectonic plate was subtracted. The first of these in-situ observations, commenced in 2001 (47. RAE), were restricted to the southern part of Lake Vostok [31]. The participation of geodesists in the continental traverses conducted by RAE allowed extending these observations to the central and northern parts of the lake [22]. To date (including observations up to 2011, 56 RAE), surface flow velocities are determined for a total of 50 markers in the Lake Vostok region (Fig. 1). The accuracy of the velocity components depends essentially on the time span between the first and the last observation on the marker. For all of the 50 markers this time span amounts to one year or more; and accuracies of typically 10 mm/a (flow velocity) and 0.5° (flow direction) were achieved [22].

The observed ice-flow velocities were used to validate ice-flow models in the Lake Vostok region. At present, ice-dynamic models [18, 27] poorly predict the flow velocity field over the subglacial lake. On the other hand, especially in the southern part of the lake, the flow velocity directions derived from the GNSS observations agree well with the flow trajectories inferred by structure tracking from radio-echo sounding data [28]. The surface velocities observed on GNSS markers along the flow line through Vostok station (VFL; e.g. [12]) were also used to derive constraints for the transit time of an ice particle across the lake and the rate of basal ice accretion [22, 31].

Furthermore, the observed velocity components form the basis for the determination of horizontal deformations at the surface of the ice sheet by means of a strain analysis [20]. Around Vostok station, a polygon of GNSS markers was established and four times (2001–2011) observed for a detailed monitoring of the surface deformations in the surroundings of the 5Г drilling site [31]. Our results indicate that the surface deformation in the area of Vostok station is characterized by extension both along and across the ice flow direction. This agrees with the large scale surface deformations observed in the southern part of the lake, and there are no indications for an additional local effect around Vostok station, e.g. related to the 5Г borehole. The flow velocities and deformation rates derived from the GNSS observations were combined with ice thickness data inferred from radio-echo sounding [6] and glaciological data to determine the local ice mass balance at Vostok station [20]. For the area of the deformation polygon, a change of the ice mass over time close to zero was revealed.

Surface height changes. The observation of changes in the surface height over Lake Vostok allows conclusions not only about the ice sheet, but also about the hydrological regime and hydrodynamic processes in the subglacial aquifer. GNSS observations on seven markers in the area of Vostok station between 2001 and 2007 were used to determine vertical velocities [20]. These velocities are in the order of −6 cm/a, and represent the downward motion of an ice particle (to which the marker is attached) as a consequence of the snow densification. Considering the observation accuracy, these vertical velocities are, on average, compensated by the surface accumulation rate independently derived for the last 200 years from snow pits in the Vostok station area [11]. This implies that the secular height change rate of the surface of the ice sheet is statistically not significantly different from zero [20]. In connection with the close-to-balance state of the ice sheet, revealed by the local mass balance estimate, it is concluded that no observational evidence is found for secular changes of the water level of the subglacial aquifer.

Two independent geodetic observation techniques, continuous GNSS observations over several days and interferometry based on satellite synthetic aperture radar data (SAR interferometry), were used to determine periodic and short-term surface height changes over Lake Vostok resulting from the astronomic tides in the subglacial lake and the differential effect of atmospheric pressure variations [30]. The tidal forcing generates a water circulation within the subglacial lake which manifests itself as periodical vertical displacements of the ice sheet surface in space and time in the order of up to 1 cm. Changes in the air pressure gradients over the lake produce also a response of the water masses, and thus the floating ice sheet, according to the differential effect of the local inverse barometer. This implies short-term (typically a few days) vertical sur-

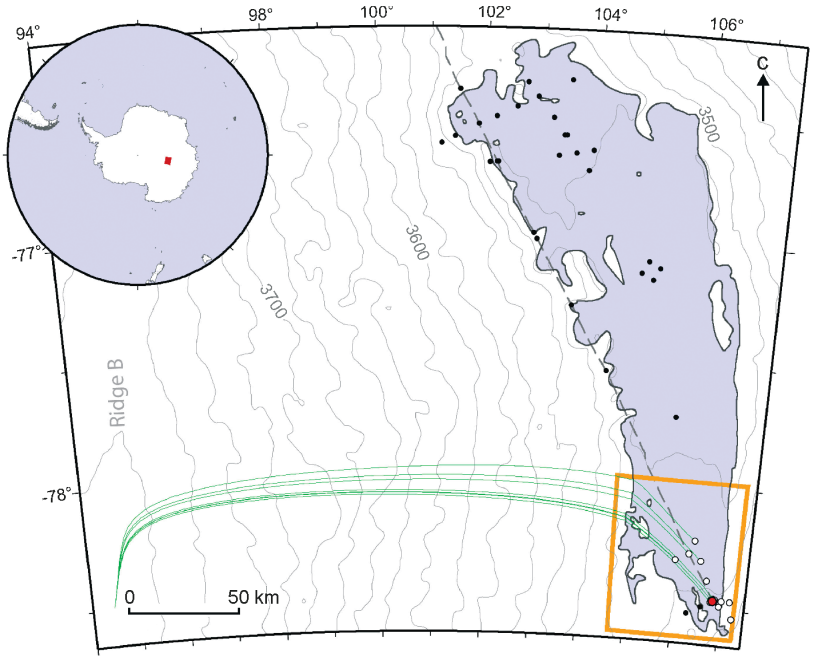

Fig. 1. Map of the Lake Vostok – Ridge B region. The area of subglacial Lake Vostok according to [5] is shown in blue. Black dots depict GNSS markers, for which ice flow velocities were determined [22]; open circles denote GNSS markers considered in the present study; the red dot shows the GNSS marker at Vostok station; green lines show modelled ice-flow lines through GNSS markers. The orange rectangle marks the area shown in Fig. 2. Height contours (20 m equidistance) are taken from [7]. In the inset, the red spot shows the area under investigation in East Antarctica

Рис. 1. Карта района подледникового озера Восток и ледораздела B.

Область распространения водной поверхности оз. Восток показана голубым цветом по данным [5]. Чёрными кружками показаны вехи GNSS (Global Navigation Satellite System), которые уже использовались для определения скорости движения льда [22]; белыми кружками – вехи GNSS (красный: станция Восток), данные по которым обсуждаются в настоящей работе; зелёными линиями обозначены модельные линии тока льда, проходящие через вехи GNSS. Оранжевый прямоугольник ограничивает изученную область ледника, которая детально показана на рис. 2. Изогипсы поверхности ледника (сечение 20 м) проведены по данным [7]. На врезке красной точкой показано положение района исследований в Восточной Антарктиде

face displacements reaching 1 to 2 cm. Since the vertical displacements produced by tides and the inverse barometer effect are restricted to the area where the ice sheet is floating, the spatial pattern of these displacements, as revealed in the SAR interferograms (Figs. 8, 9 in [8]), contains information on the extent and location of the subglacial aquifer. In fact, the configuration of peninsulas and details of the shoreline in the northern part of Lake Vostok could be predicted based on these interferograms, already before they were confirmed by the results of ground-based radio-echo sounding [5].

Observations and data

Horizontal velocity components derived from repeated GNSS observations on surface markers in the south-eastern part of subglacial Lake Vostok form the basis for the present study. They represent a subset of the ice-flow velocities presented by Richter et al. 2012 [22]. In the following, we will focus on the 12 GNSS markers highlighted in Fig. 1, and shown in more detail in Fig. 2. One of these markers (1 in Fig. 2) is located within the territory of Vostok station, about 70 m away from the 5Г drilling site. The markers 2 and 3 are part of the deformation polygon around Vostok station [20, 31]. The markers 1–9 were installed and first observed in the Antarctic field season 2001/02. In the following season, these markers were re-occupied and marker 10 was observed for the first time. All these markers consist of wooden stakes, 80 cm long, buried about 50 cm deep into the snow, with a screw on top onto which the GNSS antenna is mounted during the observation [31]. Each of these markers was complemented by two wooden reference stakes. Before and after the GNSS occupations the stability of the GNSS marker was checked by tape and levelling measurements within the triangle. The occupations usually lasted for several days to weeks, at minimum 24 h. In early 2007 marker 11, and one year later marker 12 were installed and observed. These two markers consist of aluminium tubes of 75 cm length, on top of which the GNSS antenna is mounted via an adapter. Since 2007 most of the markers (except markers 7 and 8) were re-occupied. Table 1 gives a summary of the GNSS markers and their occupations. During the occupations, a geodetic GNSS antenna was mounted on the marker and dual-frequency GPS (and in some cases also GLONASS) code and phase measurements were recorded. The antenna orientation was documented and introduced in the data analysis.

For the GNSS data processing the Bernese GPS Software was used. Based on the collected GNSS observation

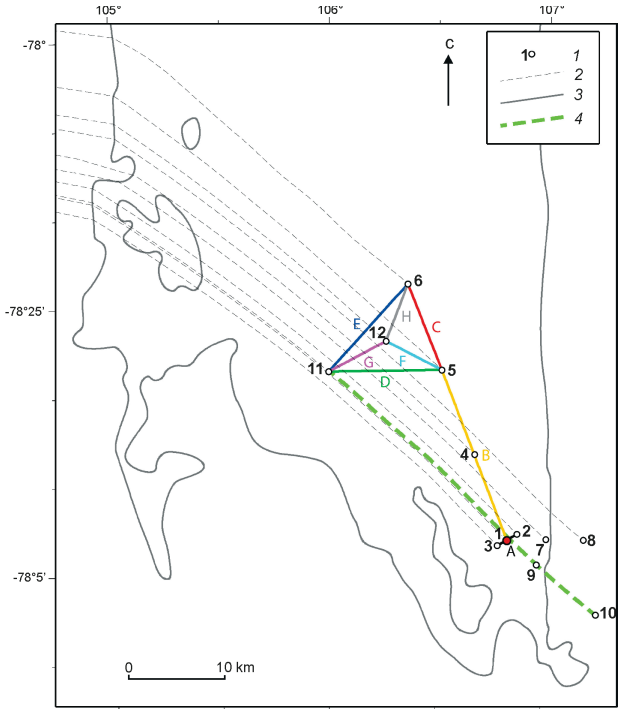

Fig. 2: Map of the region under investigation, the southern part of subglacial Lake Vostok.
1 – GNSS markers considered in this study, numbers according to Table 1; *2* – modelled upstream ice-flow lines through the GNSS markers; *3* – shoreline of subglacial Lake Vostok [5]; *4* – segment of the flow line through Vostok station (VFL). The coloured lines depict the analyzed flux gates between pairs of GNSS markers, letters according to Table 2. The red dot shows the GNSS marker at Vostok station

Рис. 2. Карта района исследований в южной части подледникового озера Восток:
1 – вехи GNSS, использованные в настоящей работе (номера вех как в табл. 1); *2* – модельные линии тока льда, проходящие через вехи GNSS; *3* – береговая линия оз. Восток [5]; *4* – участок линии тока VFL, проходящей через станцию Восток. Цветные прямые – створы ледяных потоков, для которых проводились балансовые расчёты между соответствующими вехами GNSS (буквенные обозначения створов как в табл. 2)

data, and including in addition data from 14 permanent GNSS stations distributed around the Antarctic continent, 3D coordinates and velocities were determined for each marker with respect to a global terrestrial reference frame. Details on the GNSS data processing, the coordinate determination, the reference frame and the assessment of the accuracy of the results are given by [3, 22]. The horizontal velocity components of the markers in the Lake Vostok region were corrected for the effect of the rotation of the Antarctic tectonic plate. The resulting horizontal velocities represent therefore the surface ice-flow velocity relative to bedrock. The ice-flow velocities and ice-flow azimuths obtained for the 12 markers under investigation, along with their uncertainties are included in Table 1.

In addition to the ice-flow velocity vectors for the GNSS markers, height profiles of the ice sheet were derived from kinematic GPS observations during scientific traverses [4]. In this study, we use in particular the surface height profile determined along a segment of the flow line through the drilling site at Vostok station (VFL, see e.g. [12]). The results of the geodetic observations are complemented by ice thickness data derived from ground-based radio-echo sounding [6]. The accuracy of a single ice thickness value in the vicinity of Vostok station has been estimated at 13 m, composed of a systematic uncertainty of 11.2 m and random measurement noise of 5.7 m [20]. This estimate has been confirmed recently by the total thickness of the vertical ice column of 3759 m derived after the penetration of the 5Г bore hole into the lake. Throughout the Lake Vostok region, a crossover analysis of all the thickness profiles derived from ground-based radio-echo sounding yielded a standard deviation of 42 m. This data set was merged with ice thickness data derived from airborne radio-echo sounding to a gridded ice thickness model [26] (crossover standard deviation including both data sets: 65 m). Furthermore, the high-resolution shoreline of the subglacial aquifer inferred from radio-echo sounding is used [5].

In addition, glaciological data on the surface accumulation, basal accretion and the snow/firn/ice density were introduced in the analysis. Ekaykin et al. [12] present surface accumulation rates along the VFL 100 km upstream from Vostok station. In addition to results of accumulation stake measurements, long-term mean accumulation rates representative for the last 50 or more years were derived from three snow pits and shallow ice cores along this flow line segment (see also [2]). For the last 200 years, the mean surface accumulation rate at Vostok station amounts to 20.6±0.3 mm/a water equivalent (w.e.) [11]. Practically the same, constant value (21 mm/a w.e.) was adopted for the VFL segment extending from 26 km upstream to 12 km downstream from Vostok station, which is a subject of the present study. Stake farm measurements at Vostok station over the last 40 years yielded an accumulation rate of 22.9±1.8 mm/a w.e. [11].

Information on the variation in the thickness of basal accretion ice along the VFL can be derived from the results of airborne radio-echo sounding [8]. These data indicate an accretion ice thickness of 120 m for the location 16 km downstream from the bedrock ridge/island off the western lake shore (33 km NW from Vostok station); 180 m at Vostok station; and 250 m at the intersection of the VFL with the downstream (eastern) lake shore. These values seem to underestimate the accretion thickness by about 50 m. According to the 5Г ice core, an accretion thickness of 230 m at Vostok station follows from the depth of the interface meteoric-accreted ice of 3529 m [15] and the total thickness of the vertical ice column of 3759 m. Applying the 50 m offset we obtain a 170 m accretion thickness for the upstream location 16 km SE from the bedrock ridge. For the location of re-grounding of the VFL this yields an accretion thickness of 300 m, which is in good agreement with the 295 m stated by Bell et al. 2002 [8] as the average accretion ice thickness along the south-eastern lake shore. Considering Fig. 4 in [8] and using the latter thickness value as well as the «corrected» values for Vostok station and the upstream location, we infer

*Table 1. Ov***erview of the GNSS markers.**
Their numbers according to Fig. 2, their coordinates, the year of the first and last observation, the number of occupations, the total amount of observation data (in daily files), the inferred total ice-flow velocity v with its uncertainty estimate σ_v (in mm/a), and the ice-flow azimuth α with its uncertainty estimate σ_α (in degree NESW) are given

№	Latitude S		Longitude W		Observation	Occupations	Observation data, d	$v \pm \sigma_v$, mm/a	$\alpha \pm \sigma_\alpha$
1	78°	27.962'	106°	49.966'	2001–2010	5	148	1994±1	134±0.1°
2	78°	27.586'	106°	52.791'	2001–2009	4	16	1994±1	133±0.1°
3	78°	28.252'	106°	47.302'		4	11	1992±1	134±0.1°
4	78°	23.146'	106°	40.594'	2001–2002	2	12	1894±10	134±0.3°
5	78°	18.407'	106°	31.252'		2	6	1793±9	133±0.3°
6	78°	13.582'	106°	21.681'	2001–2010	4	71	1661±1	132±0.1°
7	78°	27.871'	107°	0.896'	2001–2002	2	10	2019±10	132±0.3°
8	78°	27.871'	107°	11.431'		2	95	2041±8	128±0.2°
9	78°	29.302'	106°	58.381'	2001–2006	3	33	2029±2	132±0.1°
10	78°	32.070'	107°	15.276'	2002–2006	3	24	2087±2	128±0.1°
11	78°	18.530'	105°	59.838'	2006–2009	3	5	1659±7	129±0.2°
12	78°	16.810'	106°	15.702'	2007–2009	2	3	1737±10	131±0.4°

the accretion ice thickness for an arbitrary point of the VFL segment under investigation by linear interpolation.

According to Ekaykin et al. [1], the average density of the uppermost 20 cm snow layer at Vostok station amounts to 330 kg m^{-3}. From the 5Г ice core a vertical firn/ice density profile of the upper 2540 m was derived [17]. In the following, we assume the uppermost 2000 m of this profile as representative for the region under investigation. For the part of the ice column below 2000 m, we adopt a constant density derived from the mean of the profile values between 2000 m and 2540 m depth (923 kg m^{-3}).

Interpretation and Discussion

Mean surface accumulation rates. Richter et al. [22] applied the flux gate method (e.g. [10]) to derive mean accumulation rates for four surface segments between Ridge B and the western shore of the northern part of Lake Vostok. The same method is now applied to the area of Vostok station and the southern part of Lake Vostok. This approach is based on the assumption of steady state. Richter et al. [20] have shown that the ice mass in the vicinity of Vostok station is at present close to balance and hence have justified this assumption. In this case the ice mass passing during a given time interval through a flux gate, e.g. between two GNSS markers, must equal the mass of snow accumulating during the same time interval over a surface segment bounded by the flux gate and the flow lines through the markers up to the ice divide. Thus, knowing the ice-flow velocity at the flux gate, the ice thickness Z along the flux gate, and the mean density ρ of the vertical ice column at the flux gate, the mean net accumulation rate a for this surface segment can be determined according to

$$A_s a = A_v Z \rho. \quad (1)$$

Here, A_s denotes the surface area of the surface segment between the flow lines and A_v the surface area of flow advance. Assuming a linear change in the flow velocity and flow direction between the two markers, A_v represents a quadrangle made up of the positions of the two GNSS markers (flux gate) at the beginning and at the end of the considered time interval, respectively. Considering a time interval of one year, it is determined by the coordinates and horizontal velocity vectors (unit m/a) derived for the markers from the GNSS observations. For the floating part of the ice sheet above Lake Vostok the observed surface velocities can be regarded as representative for the entire ice column due to the absence of basal friction. The excellent agreement of flow trajectories inferred by structure tracking from internal layers at different depths with surface flow directions derived from GNSS observations confirms this assumption. Therefore, GNSS markers on grounded ice or close to the grounding line were not considered in this analysis. The GNSS markers and the corresponding flux gates are shown in Fig. 2.

In (1) Z stands for the thickness of the meteoric ice. Therefore, in the southern part of Lake Vostok, the thickness of the basal accreted ice must be subtracted from the total ice thickness values. For the markers close to Vostok station (1–3), the total ice thickness was derived from the radio-echo profile presented in [20] and the accretion thickness according to the 5Г ice core (230 m, Section 3) was adopted. For the remaining markers, the accretion thickness was inferred from the VFL accretion thickness model (Section 3) after projecting their positions orthogonally to the flow direction onto the VFL profile. In 100 m steps along the flux gate, the total ice thickness was extracted from the gridded ice thickness model by [26] and the local accretion ice thickness obtained by linear interpolation between both markers was subtracted. At each step, also the mean density of the meteoric ice column ρ was determined by integrating the vertical density profile (Section 3) from the surface down to the base of the meteoric ice. The mean values for the meteoric ice thickness and its density was then obtained by integration along the flux gate.

The introduction of the surface segment area A_s in (1) requires the determination of the upstream flow lines through the markers. In general, the flow lines can be inferred from an ice surface DEM by following the maximum surface gradient

Table 2. Flux gates in the southern part of Lake Vostok.
For the flux gates shown in Fig. 2, the involved GNSS markers, the inferred mean surface accumulation rate a with its formal uncertainty estimate σ_a (in mm/a w.e.; equivalent with kg/m^2), the surface area A_s of the upstream surface segment and the annual mass flux is given

Flux gate	GNSS, markers		$a \pm \sigma_a$, mm/a w.e.	A_s, km^2	Mass flux, 10^9 kg/a
A	2	3	23.0±1.1	645.5	14.839
B	1	5	22.4±2.5	2279.8	50.980
C	5	6	21.9±2.4	1123.2	24.581
D	5	11	21.8±1.6	2129.3	46.480
E	6	11	21.9±1.0	3198.2	69.953
F	5	12	19.4±3.6	528.4	10.264
G	11	12	23.1±1.2	1582.1	36.943
H	6	12	21.2±1.1	1630.0	34.636

from the marker position up to the ice divide. However, over Lake Vostok, where the ice surface slope is only very small and diverging from the flow direction, this approach would not provide satisfactory results. Therefore, the flow azimuths obtained for the GNSS markers and from the flow trajectories derived by structure tracking [28] were interpolated onto a regular grid. According to this model and departing from the observed flow azimuth of the marker, the flow lines were propagated up to the western lake shore (see Fig. 2). From there on, the flow lines were derived from the DEM [7], which has been shown to be accurate within a few meters in the upper part of the ice sheet [4]. The DEM was smoothed applying a 100 km Gauss filter prior to the application of the maximum gradient tracking algorithm [10]. The flow lines, tracked from the GNSS markers on the southern part of Lake Vostok up to the point on Ridge B where the flow lines converge, are shown in Fig. 1. These flow lines, initially given in geographic coordinates, were transformed into plane coordinates applying the equal-area Mollweide projection, before the surface area of the segments was computed. Test computations applying different DEM's, different filter parameters, and different equal-area projections have revealed that the aforementioned configuration yields the most reliable results [22].

The mean accumulation rates obtained for the flux gates are given in Table 2. Their formal uncertainty estimates, included in Table 2, were obtained by propagating the uncertainties of the surface segment area (5% of A_s), of the meteoric ice thickness (50 m, including 48 m uncertainty of the adopted accretion thickness, 12 m systematic error and 5.7 m random error of the total ice thickness derived from radio-echo sounding), the flow velocity vectors (10 mm/a), the marker coordinates (10 mm), and the adopted density value (1 kg m^{-3}). In the northern part of Lake Vostok, the accuracy of the A_s, derived by the same approach adopted here, has been shown to be better than 5% (on average below 2%). However, we decided on the more conservative estimate, because the flow lines through the southern part of the lake are longer than in the north (implying a higher sensitivity of the results to uncertainties in the flow line modelling) and the flow line determination across the lake may introduce an additional uncertainty. The uncertainty contribution of the A_s dominates by far (factor 10) the error budget.

In general, the mean accumulation rates obtained for the different flux gates are very similar among themselves. Since substantial differences in the mean accumulation rates should not be expected over such a relatively small area, this fact may suggest the consistency of our results. Also the uncertainty estimates are quite homogeneous. The largest formal uncertainties are obtained for those flux gates which intersect the flow lines in a narrow angle (F, B, C). The internal agreement among the results for the flux gates D–H confirms the consistency of the results as well as the accuracy estimates. Flux gate A, centred at Vostok station, is the smallest flux gate. For this gate we possess the most accurate and reliable information on the thickness of the meteoric and accreted ice, on the vertical density profile and on the flow velocities. Moreover, the assumption of a linear change of the ice flow vector and the accretion ice thickness between the two markers seems most justified over such a short distance. On the other hand, this small flux gate is also more sensitive to small deviations from the modelled flow lines.

The accumulation rates given in Table 2 would represent the present-day net surface accumulation, if the ice sheet would respond immediately to changes in the accumulation. However, according to estimates of the relaxation time of the East Antarctic ice sheet (e.g. [29]), it may take up to 10 ka for accumulation changes to manifest themselves in the observed ice mass flux. A comparison of the flux gate results with present-day accumulation rates derived from glaciological in-situ investigations thus implies that the steady-state assumption is valid during the Holocene. It also implies that the flow lines would not have changed significantly during this time. The agreement of the paleo-flow trajectories derived by [28] with the present-day flow directions determined by GNSS observations [22] suggests that at least over the southern part of Lake Vostok the ice flow direction has not changed significantly since the structures identified in the internal layers were formed at the western lake shore (in the order of 50 ka BP, cf. [24]).

The two flux gates most representative for Vostok station (A, G) both reveal a flux equivalent to a mean accumulation rate of 23 mm/a w.e. This is slightly higher than the accumulation rate of 20.6 ± 0.3 mm/a w.e. derived at Vostok station for the period 1816–2004. Accumulation stake measurements (2005–2012) along the VFL profile 107 km upstream from Vostok station indicate a slightly increasing accumulation towards W as well as substantially increased accumulation rates within profile sections of concave surface curvature [12]. Furthermore, the accumulation rates at Ridge B are expected to be higher than at Vostok station [24]. It must be noted that the accumulation near the ice divide contributes to the presented mean rates with a smaller weight than the accumulation close to the flux gate, because they are represented within the segment by a smaller fraction of the surface area due to the generally divergent flow down from the ice divide. Altogether, the results obtained for flux gates A and G are consistent with the long-term accumulation rate at Vostok station and the spatial variation of the accumulation along the flow line upstream.

This gives confidence in the applicability of the flux gate approach and that the steady-state assumption is reasonable.

The results obtained for the remaining flux gates might suggest a slight decrease in accumulation towards N. This would not be expected from flux gate observations in the northern part of the lake [22] and from glaciological data within the lake area [2, 12]. If the trend apparent in the flux gate results was real, the latter alone would not allow a detailed localization of spatial accumulation anomalies within the segments, e.g. to distinguish between the lake area and the vicinity of the ice divide. However, in the comparison of the flux gate results their uncertainties have to be kept in mind. In particular, the accretion thickness away from the VFL is poorly constrained by observational data. Therefore, we do not interpret the flux gate results as an indication for a decrease of the mean accumulation rates towards N.

Ice-flow dynamics across the transition zone. The ice surface topography above Lake Vostok is characterized by prominent troughs along the western grounding line and bumps along the eastern grounding line, bounding the flat ice surface of the freely floating part of the ice sheet [13, 19]. These features have been interpreted as the manifestation of changes in the ice flow dynamics in the zones of transition from grounded to floating (western shore) and back to grounded ice (eastern shore) connected to changes in the ice-base conditions in these zones [19]. At the upstream (western) grounding line, the vanishing basal friction induces a local speed-up of the ice flow which results in a thinning of the ice sheet and thus in a local negative topographic anomaly. At the opposite lake shore occurs the reverse process: increase in basal friction, slowdown of the ice flow, thickening of the ice sheet and a positive topographic anomaly. Based on a high-resolution DEM of the ice sheet surface and reasonable assumptions on the ice thickness, flow velocity, accumulation rate and the basal sheer stress, Rémy et al. [19] attempted to explain these peripheral topographic features by means of a first-order model of the changing ice flow throughout the transition zone. Applying the steady-state equation, and assuming a linear decrease (western shore) of the basal sheer stress over 10 km, a satisfactory agreement with the observed surface geometry was achieved.

Today, having accurate in-situ observations of the ice-flow velocity [22, 31], ice thickness [6], accumulation rate [12], grounding line position [5] and the surface topography [4, 13] at hand, one might hope to be able to invert this approach in order to gain insights into the basal shear stress around Lake Vostok. For this purpose, we choose the segment of the VFL from 26 km upstream to 12 km downstream from Vostok station which traverses the transition zone at the south-eastern (downstream) lake shore. Along this flow line segment, we can rely on four repeatedly observed GPS markers (1, 9, 10, 11; see Fig. 2). The course of the flow line within this interval was inferred from the gridded model of flow azimuths (Section 4.1) starting from GPS marker 9 (closest to the grounding line). In fact, the other three markers are aligned very closely along this flow line, their lateral offsets amount to 74 m (marker 11), 302 m (1), and 23 m (10). Available continuous profiles of the ice thickness, derived from ground-based radio-echo sounding [6], and of the surface height, derived from kinematic GPS observations [4], diverge laterally only slightly (at most 1 km) from this flow line and were projected orthogonally onto the improved profile course. The surface height profile, extending only from Vostok station downstream, was complemented in the upstream part by surface heights interpolated from the hybrid DEM by [13]. The surface height profile and the ice thickness profile are shown in Fig. 3, *a*. For the entire profile length a constant accumulation rate of 21 mm/a w.e. is assumed, according to the long-term accumulation rate profile given by [2, 12] for the VFL upstream from Vostok station. The basal accretion rate distribution along our profile was derived from the VFL accretion ice thickness model (Section 3, see Fig. 3, *b*). It implies an increased accretion rate between Vostok station and the grounding line, and zero accretion beyond.

Between the four GPS markers along the profile, the ice-flow velocity was linearly interpolated (see Fig. 3, *b*). The flow velocity vectors observed at the remaining GPS markers included in Fig. 2, off but close to the profile, were used to derive the across-flow strain component (convergent/divergent flow; see Fig. 3, *c*). In this way, all these quantities are given at equidistant 50 m intervals along the improved flow line. The surface height profile shown in Fig. 3, *a* confirms the symmetry of the peripheral bump and its dimensions (20 km length, 6 m height) as stated by [18]. This marks the transition zone where we will focus our interest on.

We slightly extend the formal approach of [19] by including the across-flow strain component dV/dy in the mass conservation equation and adding the basal accretion rate b to the surface accumulation rate a (both a and b in unit m/a ice equivalent) [14]:

$$a + b - (UdZ/dx + ZdU/dx + ZdV/dy) = E + dZ/dt. \quad (2)$$

Here, U denotes the ice-flow velocity along the flow line, dU/dx the along-flow strain (extension/compression), Z the ice thickness, and dZ/dx the ice thickness gradient along the flow line. The right-hand side of (2) is composed of the combined effect of modelling and observation uncertainties of all involved quantities E and the change in the surface height over time dZ/dt reflecting the ice-mass balance. For each data point along the profile, (2) is evaluated. The resulting variation of the $(E + dZ/dt)$ quantity along the profile is shown in Fig. 3, *c* (red curve).

For the upstream part of the profile, down to the grounding line, this quantity varies only slightly and remains close to zero. Exactly at the grounding line, a sharp increase by approximately 50 cm/a is observed. Further down the flow line, the $(E + dZ/dt)$ drop and oscillate with large amplitudes, apparently in correlation with the ice thickness gradient dZ/dx. This striking change in the behaviour of the $(E + dZ/dt)$ is not expected. A temporal change in the surface height dZ/dt is assumed to be coupled with climatically-induced ice-mass changes, which should occur uniformly over regional scales. An interpretation of the red curve in Fig. 3, *d* as real spatial variation of the surface height change rate dZ/dt is therefore not plausible. On the other hand, the sudden increase in the

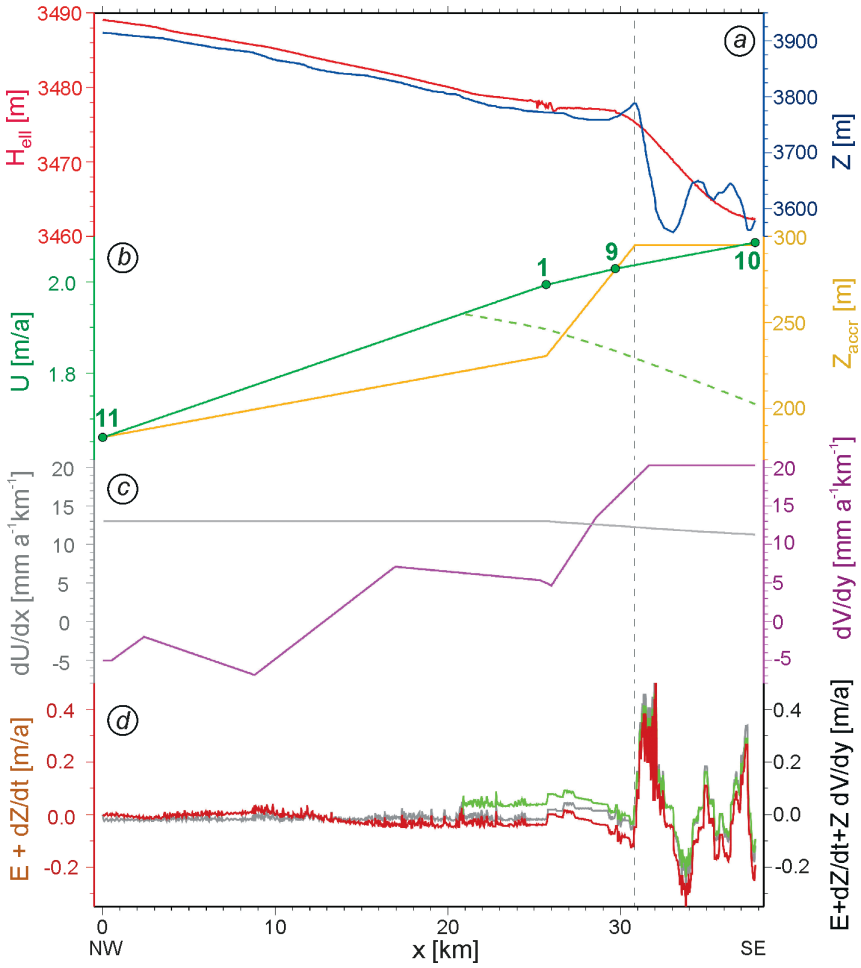

Fig. 3. Profile along a segment of the flow line through Vostok station (VFL; see Fig. 2): *a* – the red line indicates the ellipsoidal height H_{ell} of the ice surface over the profile distance *x* from marker 11 to marker 10; the blue line shows the ice thickness *Z*. The vertical dashed line indicates the location of the grounding line as detected by terrestrial radio-echo sounding; Vostok station is located at $x = 25.7$ km (marker 1); *b* – green dots: ice-flow velocity *U* observed at the four GNSS markers 11, 1, 9, 10; green line: continuous flow velocity profile obtained by interpolation between the markers; dashed green line: hypothetical flow-velocity profile assuming slowdown in the transition zone due to basal friction; yellow line: model of the accretion ice thickness Z_{accr} along the profile; *c* – grey line: along-flow surface deformation dU/dx ($dU/dx < 0$: compression; $dU/dx > 0$: extension); purple: across-flow surface deformation dV/dy ($dV/dy < 0$: convergence; $dV/dy > 0$: divergence); *d* – modelling results. Red line: Sum of observation and modelling uncertainties and temporal surface height change $(E + dZ/dt)$; green line: the same when assuming the hypothetical flow-velocity profile (dashed green line above); grey line: the same as the red line, without accounting for the effect of across-flow surface deformation $(E + dZ/dt + ZdV/dy)$

Рис. 3. Характеристики исследованного участка линии тока льда VFL, проходящей через станцию Восток (см. рис. 2):

a – красная линия – высота поверхности ледника H_{ell} (относительно эллипсоида WGS84) между вехами *11* и *10* (*x* – расстояние по профилю от вехи *11*); голубая линия – мощность ледника *Z*. Вертикальный пунктир показывает положение линии налегания ледника по данным наземного радиолокационного зондирования. Станция Восток (веха 1) расположена на расстоянии $x = 25{,}7$ км от вехи 11; *b* – зелёными кружками показаны значения скорости движения льда *U*, измеренные на четырёх вехах GNSS с номерами 11, 1, 9, 10; зелёная линия – непрерывный профиль скорости движения льда, полученный путём интерполяции между вехами; зелёный пунктир – гипотетический профиль, учитывающий замедление скорости течения льда вблизи линии налегания в результате появления трения на контакте ледник–подстилающие породы; жёлтая линия – расчётная мощность озёрного льда Z_{accr} на данном профиле; *c* – серая линия – продольная (вдоль линии тока) деформация поверхности ледника dU/dx; пурпурная линия – поперечная деформация поверхности ледника dV/dy; *d* – результаты моделирования: красная линия – сумма экспериментальных и модельных погрешностей и возможных временных изменений высоты поверхности ледника $(E + dZ/dt)$; зелёная линия – то же, но без учёта эффекта поперечных деформаций поверхности ледника $(E + dZ/dt + ZdV/dy)$

variation range at the grounding line can also not be explained as an effect of observation and modelling uncertainties *E*, since the observation techniques and data sources used are exactly the same to either side of the grounding line. The inclusion of the across-flow strain dV/dy has only little impact on the model output as becomes evident by the grey curve in Fig. 3,*d*. It shows the evaluation of (2) neglecting the across-flow strain on the left-hand side and thus the combined effect of $(E + dZ/dt + ZdV/dy)$. However, the difference with respect to the red curve (complete model including across-flow strain) is only marginal.

We interpret therefore the increase of the $(E + dZ/dt)$ at the grounding line as an indication that an important element is still missing in the modelling approach in (2) and [19]. It can be concluded that the modelling approach in its present formulation is not suited to derive the basal shear stress downstream from the grounding line. In fact, the inclusion of basal friction in the model would imply a decrease in the ice-flow velocity downstream from the grounding line. However, a steady increase of the surface flow velocity is observed along the entire profile, including also marker 10 located 7 km downstream from the lake shore. Surface velocities observed on grounded ice generally overestimate the mean velocity of the vertical ice column. Usually a factor of 0.9 is applied to derive velocities representative for the ice column from observed surface velocities (e.g. [10]). In a test computation we reduce the effective flow velocity by multiplication of the surface velocity with a factor decreasing linearly from 1 (10 km upstream from the grounding line) to 0.8 (10 km downstream from the grounding line, cf. [19]). This hypothetical flow velocity profile is included in Fig. 3, *b* (green dashed line). The $(E + dZ/dt)$ resulting from (2) with *U* and dU/dx taken from this hypothetical velocity profile are depicted by the green line in Fig. 3, *d*. The decrease in the flow velocity results in an immediate increase of the $(E + dZ/dt)$, where the velocity scaling begins, and follows thereon roughly parallel to the red curve. Thus, an inclusion of basal friction and velocity decrease in the modelling would not reduce the increase of the $(E + dZ/dt)$ at the grounding line.

The most poorly constrained parameter in our analysis is probably the transversal strain dV/dy (purple line in Fig. 3, *c*). It represents the variation in the flow-tube width along the flow line. For grounded ice, where the ice bed relief becomes effective, larger changes in the divergence/convergence of flow over short distances can be expected. It is clear that the adopted linear interpolation along the profile is only a crude approximation of the variation of the transversal strain, in particular where the ice is grounded. Part of the striking oscillations of the ($E + dZ/dt$) at the grounding line and beyond might thus be attributed to the limited resolution of this parameter along the profile. On the other hand, the representation of the transversal strain in Fig. 3, *c* relies on in-situ observations at eight points along the profile. Within 4 km to either side of the grounding line the transversal strain is constrained by three observed values, one of them located exactly at the location of the pronounced peak of the ($E + dZ\,dt$), about 2 km downstream from the grounding line. This peak can therefore not be explained by the uncertainty of the transversal strain.

The suspicion, that the model description of the flow dynamics in the transition zone is not yet complete, is qualitatively confirmed also by two profiles across the north-western lake shore (profiles **a** and **b** in [22]). There, where the vanishing basal friction is thought to generate a speed-up of the ice flow [19], a steady decrease of the flow velocity towards the lake centre is observed.

Conclusions

The position of the drilling site at Vostok station, far away from the ice divide, poses particular challenges for the interpretation of the 5Г ice core [24]. On the other hand, its location above the largest of the Antarctic subglacial lakes can be considered as a fortunate coincidence. Due to this fact unique insights become possible which would not be feasible on grounded ice, for example the reconstruction of paleo-flow trajectories or the determination of the present-day mass balance. Geodesy can make useful contributions to the interpretation of the ice core data and to the understanding of the glaciological setting of the Lake Vostok system (e.g. strain rates around the drilling site, accurate ice-flow velocities for the inference of transit times, accretion rates and water residence times).

Based on observed ice-flow velocities and the flux gate method, mean net surface accumulation rates are presented which are representative for surface segments extending from the southern part of Lake Vostok to the Ridge B ice divide. These results are consistent with the present-day accumulation rate at Vostok station and its along-flow variations upstream and suggest that the region under investigation has been close to steady state during the Holocene. One important component of the ice core interpretation consists in a precise reconstruction of the ice-flow velocity field for the Lake Vostok-Ridge B region in the present and past. Existing glacio-dynamic models have been shown to be unable to predict sufficiently well the flow velocities and directions over Lake Vostok [22]. By means of an analysis of a segment of the VFL crossing the grounding line downstream from Vostok station, the importance of the transition zone for the regional flow field as well as conceptual deficiencies in current modelling approaches were identified. A better understanding of the mechanics of the ice flow within the transition zones is crucial for the improvement ice-flow models both for the past and present.

Acknowledgements. We sincerely thank the participants of the 47, 48, 52, 53, 55 and 56th Russian Antarctic Expedition, in particular the staff at Vostok station and the scientific traverses, for their valuable support of the field work.

The field work was partly funded by the German Research Foundation DFG (grants DI473/34-1, DI473/38-1) and the Russian Foundation of Basic Research (grant 10-05-91330-NNIO-a).

References

1. *Екайкин А.А., Липенков В.Я., Петит Ж.Р., Массон-Дельмотт В.* 50-летний цикл в изменениях аккумуляции и изотопного состава снега на станции Восток // МГИ. 2003. Вып. 94. С. 163–173.
2. *Екайкин А.А., Шибаев Ю.А., Липенков В.Я., Саламатин А.Н., Попов С.В.* Гляциогеофизические исследования линий тока льда, проходящих через подледниковое озеро Восток // Полярная криосфера и воды суши: Вклад России в Международный полярный год / Под ред. В.М. Котлякова. М.-СПб.: Paulsen, 2011. С. 48–69.
3. *Матвеев А.Ю., Федоров Д.В., Гребнев В.П., Лукин В.В., Fritsche M., Richter A., Dietrich R.* Высокоточные временные ряды координат, полученные из GNSS наблюдений в Антарктиде. I: Геодезические определения // Геодезия и картография. 2012. № 11. С. 10–20.
4. *Федоров Д.В., Schröder L., Knöfel C., Richter A., Матвеев А.Ю., Гребнев В.П., Лукин В.В., Dietrich R.* Определение профилей высот поверхности ледника вдоль внутриконтинентальных трасс в Антарктиде посредством кинематических GPS-наблюдений // Лёд и Снег. 2012. № 4 (120). С. 49–56.
5. *Попов С.В., Черноглазов Ю.Б.* Подледниковое озеро Восток, Восточная Антарктида: береговая линия и окружающие водоёмы // Лёд и Снег. 2011. № 1 (113). С. 13–24.
6. *Попов С.В., Масолов А.Н., Лукин В.В.* Подледниковое озеро Восток, Восточная Антарктида: мощность ледника, глубина озера, подлёдный и коренной рельеф // Лёд и Снег. 2011. № 1 (113). С. 25–35.
7. *Bamber J.L., Gomez Dans J.L., Griggs J.A.* A new 1 km digital elevation model of the Antarctic derived from combined satellite radar and laser data. Pt. I: Data and methods // The Cryosphere. 2009. № 3 (2). С. 101–111.
8. *Bell R.E., Studinger M., Tikku A.A., Clarke G.K.C., Gutner M.M., Meertens C.* Origin and fate of Lake Vostok water frozen to the base of the East Antarctic ice sheet // Nature. 2002. V. 416. P. 307–310.
9. *Benveniste J.* Towards more efficient use of radar altimeter data // ESA Bulletin. 1993. V. 76. P. 64–71.
10. *Cuffey K.M., Paterson W.S.B.* The Physics of Glaciers. Butterworth-Heinemann, 2010. 693 P.
11. *Ekaykin A.A., Lipenkov V.Ya., Kuzmina I.N., Petit J.R., Masson-Delmotte V., Johnsen S.J.* The changes in isotope composition and accumulation of snow at Vostok station, East Antarctica, over the past 200 years // Annals of Glaciology. 2004. V. 39. P. 569–575.
12. *Ekaykin A.A., Lipenkov V.Ya., Shibaev Yu.A.* Spatial distribution of the snow accumulation rate along the ice flow lines between Ridge B and Lake Vostok // Лёд и Снег. 2012. № 4 (120). С. 122–128.
13. *Ewert H., Popov S. V., Richter A., Schwabe J., Scheinert M., Dietrich R.* Precise analysis of ICESat altimetry data and assess-

ment of the hydrostatic equilibrium for subglacial Lake Vostok, East Antarctica // Geophys. Journ. International. 2012. doi:10.1111/j.1365-246X.2012.05649.x.
14. *Horwath M., Dietrich R., Baessler M., Nixdorf U., Steinhage D., Fritzsche D., Damm V., Reitmayr G.* Nivlisen, an Antarctic ice shelf in Dronning Maud Land: geodetic–glaciological results from a combined analysis of ice thickness, ice surface height and ice-flow observations // Journ. of Glaciology. 2006. V. 52. № 176. P. 17–30.
15. *Jouzel J., Petit J.R., Souchez R., Barkov N.I., Lipenkov V.Ya., Raynaud D., Stievenard M., Vassiliev N.I., Verbeke V., Vimeux F.* More than 200 meters of lake ice above subglacial Lake Vostok, Antarctica // Science. 1999. V. 286. P. 2138–2141.
16. *Leonard K., Bell R.E., Studinger M., Tremblay B.* Anomalous accumulation rates in the Vostok ice-core resulting from ice flow over Lake Vostok // Geophys. Research Letters. 2004. V. 31. L24401. doi:10.1029/2004GL021102.
17. *Lipenkov V.Ya, Salamatin A.N., Duval P.* Bubbly-ice densification in ice sheets: II. Applications // Journ. of Glaciology. 1997. V. 43. № 145. P. 397–407.
18. *Pattyn F., De Smedt B., Souchez R.* Influence of subglacial Lake Vostok on the regional ice dynamics of the Antarctic ice sheet: a model study // Journ. of Glaciology. 2004. V. 50. P. 583–589.
19. *Rémy F., Shaeffer P., Legrésy B.* Ice flow physical processes derived from ERS-1 high-resolution map of the Antarctica and Greenland ice sheets // Geophys. Joun. International. 1999. V. 139. P. 645–656.
20. *Richter A., Popov S.V., Dietrich R., Lukin V.V., Fritsche M., Lipenkov V.Ya., Matveev A.Yu., Wendt J., Yuskevich A.V., Masolov V.N.* Observational evidence on the stability of the hydroglaciological regime of subglacial Lake Vostok // Geophys. Research Letters. 2008. V. 35. L11502. doi:10.1029/2008GL033397.
21. *Richter A., Fedorov D.V., Dvoryanenko A.K., Popov S.V., Dietrich R., Lukin V.V., Matveev A.Yu., Fritsche M., Grebnev V.P., Masolov V.N.* Observation of ice-flow vetors on inner-continental traverses in East Antarctica // Лёд и Снег. 2010. № 1 (109). С. 30–35.
22. *Richter A., Fedorov D.V., Fritsche M., Popov S.V., Lipenkov V.Ya., Ekaykin A.A., Lukin V.V., Matveev A.Yu., Grebnev V.P., Rosenau R., Dietrich R.* Ice flow velocities over subglacial Lake Vostok, East Antarctica, determined by 10 years of GNSS observations // Journ. of Glaciology. 2012.; in review.
23. *Roemer S., Legrésy B., Horwath M., Dietrich R.* Refined analysis of radar altimetry data applied to the region of the subglacial Lake Vostok // Antarctica: Remote Sensing of Environment. 2007. V. 106. P. 269–284. doi:10.1016/j.rse.2006.02.026.
24. *Salamatin A.N., Tsyganova E.A., Popov S.V., Lipenkov V.Ya.* Ice flow line modelling and ice core data interpretation: Vostok Station (East Antarctica) // Physics of Ice Core Records II. Low temperature science, Supplement issue, 68. Sapporo, Hokkaido University Press, 2009. P. 167–194.
25. *Schutz B.E., Zwally H.J., Shuman C.A., Hanock D., DiMarzio J.P.* Overview of the ICESat Mission // Geophys. Research Letters. 2005. V. 32. L21S01. doi:10.1029/2005GL024009.
26. *Siegert M.J., Popov S., Studinger M.* Vostok Subglacial Lake: A Review of Geophysical Data Regarding Its Discovery and Topographic Setting // Antarctic Subglacial Aquatic Environments. AGU Geophysical Monograph Series. 2011. V. 192. P. 45–60.
27. *Thoma M., Grosfeld K., Mayer C., Pattyn F.* Ice flow sensitivity to boundary processes: A coupled model study in the Subglacial Lake Vostok area // Annals of Glaciology. 2012. V. 53 (60). P. 173–180. doi:10.3189/2012AoG60A009.
28. *Tikku A.A., Bell R.E., Studinger M., Clarke G.K.C.* Ice flow field over Lake Vostok, East Antarctica inferred by structure tracking // Earth Planetary Science Letters. 2004. V. 227. P. 249–261. doi:10.1016/j.epsl.2004.09.021.
29. *Van der Veen C.J.* Fundamentals of Glacier Dynamics. Rotterdam: A.A. Balkema, 1999. 462 p.
30. *Wendt A., Dietrich R., Wendt J., Fritsche M., Lukin V., Yuskevich A., Kokhanov A., Senatorov A., Shibuya K., Doi K.* The response of the subglacial Lake Vostok, Antarctica, to tidal and atmospheric pressure forcing // Geophys. Journ. International. 2005. V. 161. P. 41–49. doi:10.1111/j.1365-246X.2005.02575.x.
31. *Wendt J., Dietrich R., Fritsche M., Wendt A., Yuskevich A., Kokhanov A., Senatorov A., Lukin V., Shibuya K., Doi K.* Geodetic observations of ice flow velocities over the southern part of subglacial Lake Vostok, Antarctica, and their glaciological implications // Geophys. Journ. International. 2006. V. 166. P. 991–998. doi:10.1111/j.1365–246X.2006.03061.x.

Геодезические наблюдения и интерпретация скоростей течения льда в южной части подледникового озера Восток

Анализ результатов высокоточных геодезических измерений скоростей движения льда в южной части подледникового озера Восток, выполненный с привлечением данных о высоте поверхности и мощности ледника, плотности ледниковой толщи, аккумуляции снега и скорости нарастания озёрного льда на подошву ледника, позволил получить новую информацию о динамике Антарктического ледникового покрова в районе станции Восток. На основе предположения о стационарном состоянии ледника сделаны балансовые расчёты для восьми произвольно ориентированных створов ледяных потоков, проходящих в данном районе в непосредственной близости от глубокой скважины 5Г. Они позволили оценить среднюю аккумуляцию снега на площади сегментов ледникового покрова, простирающихся от южной части оз. Восток до ледораздела В. Полученные значения оказались весьма близки к современной аккумуляции снега в районе станции Восток. Выполнены детальные исследования линии тока льда VFL, проходящей через станцию Восток на участке от 26-го километра вверх по течению льда и от 12-го километра вниз по течению. Попытка интерпретации полученного набора данных с помощью усовершенствованной модели Реми [19] продемонстрировала несостоятельность последней корректно воспроизвести наблюдаемые изменения скорости движения льда в переходной зоне вблизи линии налегания ледника, соответствующей восточному берегу озера. Вопреки теоретическим ожиданиям, скорость движения поверхности ледникового покрова возрастает при выходе ледника на берег. Результаты проведённого исследования могут быть использованы для дальнейшего совершенствования моделей течения ледникового покрова, используемых для датирования ледяных кернов и палеоклиматической интерпретации полученных при их исследовании данных.